Nanoscale Advances

ROYAL SOCIETY OF CHEMISTRY

PAPER

View Article Online
View Journal | View Issue

Check for updates

Cite this: *Nanoscale Adv.*, 2020, **2**, 4639

Synthesis and catalytic evaluation of PVP–CeO_2/rGO as a highly efficient and recyclable heterogeneous catalyst for multicomponent reactions in water†

Shaheen Siddiqui and Zeba N. Siddiqui*

Received 16th June 2020
Accepted 24th June 2020

DOI: 10.1039/d0na00491j

rsc.li/nanoscale-advances

A highly efficient and eco-friendly route for the reduction of graphene oxide (GO) to reduced graphene oxide (rGO) was developed by using polyvinylpyrrolidone coated CeO_2 NPs (PVP–CeO_2) as a reducing and stabilizing agent. The resulting carbonaceous material, PVP–CeO_2/rGO, was well characterized with different spectroscopic techniques such as Fourier Transform Infrared (FTIR) spectroscopy, Scanning Electron Microscopy (SEM), Energy Dispersive X-ray (EDX), elemental mapping, Transmission Electron Microscopy (TEM), Raman spectroscopy, powder X-ray diffraction (XRD), Brunauer–Emmett–Teller (BET), X-ray Photoelectron Spectroscopy (XPS), and Thermal Gravimetric (TG) analyses. The material exhibited high catalytic potential towards multicomponent reactions for the synthesis of biologically relevant benzodiazepine derivatives in aqueous media. The efficiency of the material for the desired reaction was shown in the form of an excellent product yield (96–98%) and a very short reaction time period (7–10 min). The use of water as solvent and recyclability of the catalyst made the present protocol acceptable from a green perspective.

1. Introduction

Graphene is a 2D system with very strong sp^2 hybridized carbon–carbon bonds arranged in a hexagonal manner to form a layered structure with a high aspect ratio and a large π-electronic surface. It has some unique and remarkable properties such as exceptionally high thermal conductivity, a greater surface area, very high carrier mobility at room temperature and excellent mechanical properties.[1] Graphene is generally produced by three methods *viz.* chemical reduction of graphene oxide (GO),[2] chemical vapor deposition[3] and micro-mechanical stripping.[4] The chemical reduction of GO to rGO is a simple and large scale route but it involves hazardous reducing agents such as hydrazine,[5] $NaBH_4$,[6] dimethyl hydrazine,[7] hydroquinone *etc.*[8] Recently, the development of innovative synthetic approaches utilizing non-toxic and cost effective chemicals for the reduction of GO to rGO has attracted prime interest and as a result various environmentally benign methods have been adopted to synthesize rGO.[9–12] The incorporation of metal nanoparticles into GO sheets has become a widespread green methodology for the reduction of GO resulting in the formation of metal functionalized rGO such as Au–rGO,[13] Ag–rGO,[14] Pd–rGO,[15] W–rGO,[9] Fe–rGO,[16] Ti–rGO,[17] Mo–rGO,[18] Ce–rGO,[19] *etc.* Metal functionalized rGO materials have potential applications including stripping analysis of methyl parathion,[13] biological activities,[14] catalysis,[15,18] photoelectrochemical water splitting,[16] and sensing.[17,20] Focussing on catalytic applications, graphene based materials have been extensively used as catalysts in various organic transformations such as reduction of nitro organics,[21] oxidative C–H functionalization of tertiary amines,[22] Suzuki and Heck cross-coupling,[23] oxidative esterification of alcohols,[24] alkene hydrogenation,[25] Friedel–Crafts addition,[26a] Knoevenagel condensation,[26b] *etc.* To the best of our knowledge, there is no report of using metal functionalized rGO for the synthesis of benzodiazepine derivatives. Cerium oxide nanoparticles (CeO_2 NPs) have attracted tremendous interest in the field of science and nanotechnology because of their useful industrial and synthetic applications.[20,27–30] CeO_2 NPs owing to their acid–base and redox properties have been widely used as an efficient catalyst in various organic transformations such as dehydration of alcohols, alkylation of aromatic compounds, carbamate synthesis from CO_2, reduction of carboxylic acid, ketonization of alcohols, *etc.*[31] Different polymeric materials have been used for the stabilization of CeO_2 NPs. Polyvinylpyrrolidone (PVP) is a highly cross-linked, non-ionic,[32] and non-toxic[33] polymer containing both hydrophilic (the pyrrolidone moiety) and hydrophobic components (the alkyl group) in its structure.[34] It acts as a stabilizer by inhibiting the

Department of Chemistry, Aligarh Muslim University, Aligarh 202002, Uttar Pradesh, India. E-mail: siddiqui_zeba@yahoo.co.in; zns.siddiqui@gmail.com

† Electronic supplementary information (ESI) available: General experimental details, green metrics calculation, recycling experiment and spectral data of synthesized compounds. CCDC 1958389. For ESI and crystallographic data in CIF or other electronic format see DOI: 10.1039/d0na00491j

aggregation of NPs resulting from the repulsive forces through its hydrophobic carbon chains that extend into solvents and interact with each other.[35]

Benzodiazepine nuclei are important pharmacophoric scaffolds and constitute a special class of heterocycles with diverse biological activities such as anti-HIV-1,[36] antiviral,[37] antitumor,[38] *etc.* Besides their eye-catching biological properties, benzodiazepines have also been used as valuable synthons for various fused ring compounds such as imidazo,[39] triazolo,[40] and pyrimido-benzodiazepines.[41] Water as a solvent also contributes to green chemistry by featuring many benefits such as simplifying workup procedures, enabling the recycling of the catalyst, improving reactivity and selectivity, and allowing mild reaction conditions and protecting-group free synthesis in addition to being benign itself.[42] Taking into account the aforementioned properties of graphene based materials and in continuation of our ongoing research,[43] we herein, describe an easy route for the synthesis of PVP–CeO_2 coated reduced graphene oxide (PVP–CeO_2/rGO). The material was well characterized and used as an efficient heterogeneous catalyst for water compatible synthesis of benzodiazepine derivatives under environmentally benign conditions.

2. Experimental

2.1. Synthesis of graphene oxide (GO)

GO was synthesized using modified Hummers' method.[44] In a 250 mL RB flask, 1.2 g of graphite flakes, 0.55 g of $NaNO_3$ and 25 mL conc. H_2SO_4 were added and the resulting mixture was stirred for 30 min in an ice bath at 0–5 °C to obtain a black paste. To this mixture, 3.2 g of $KMnO_4$ was slowly added (at a rate of 1 g per 15 min) with vigorous stirring and temperature was maintained using an ice bath to avoid explosion. After complete addition of $KMnO_4$, the ice bath was removed and the reaction mixture was stirred at 35 °C for 2 h. After that, 50 mL of de-ionized water was added very slowly to the reaction mixture. Since, it is a highly exothermic process, a huge amount of heat is produced during this process and the temperature reaches around 100 °C and the colour of the reaction mixture turns brownish. After 25 min, 10 mL of 30% H_2O_2 and 100 mL warm water were added to the reaction flask and the mixture was stirred for 5 min resulting in the formation of a yellowish-brown solution. The resulting solution was filtered, treated with 5% HCl to remove impurities and subsequently washed with a copious amount of double distilled water. As obtained, the product (yellowish-brown) was oven dried at 60 °C for 14 h and re-dispersed in 100 mL double distilled water by ultrasonication for 3 h to obtain a brown colored GO dispersion. The resulting dispersion was filtered and washed thoroughly with deionized water and dried at 60 °C for 6 h to obtain a brown colored solid (GO) (yield: GO = 1.52 g).

2.2. Synthesis of PVP–CeO_2 coated reduced graphene oxide (PVP–CeO_2/rGO)

In the first step, PVP coated cerium oxide NPs (PVP–CeO_2 NPs) were synthesized by adopting a previously reported procedure with a slight modification.[45] In a typical run, $CeNO_3$ (130 mg) was dissolved in 5 mM aqueous solution (50 mL) of PVP and the mixture was heated at 105 °C for 3 h. After heating, the reaction mixture was poured into cold water and acetone (4 : 1 ratio, acetone/particle suspension) to remove excess PVP. The mixture was then centrifuged at 4000 rpm for 10 min. The yellow pellets (PVP–CeO_2 NPs) thus obtained were retained and the excess liquid was discarded (yield: PVP–CeO_2 = 0.98 g).

In the second step, the pellets were re-suspended in 100 mL double distilled water containing GO (1 g) and the resulting mixture was sonicated for 30 min at 45 °C. The yellowish brown colour of the solution turned black indicating the reduction of GO and formation of PVP–CeO_2/rGO. The obtained PVP–CeO_2/rGO was separated by centrifugation, washed with double distilled water and dried in a vacuum oven at 60 °C for 24 h (yield: PVP–CeO_2/rGO = 1.78 g).

2.3. General procedure for the synthesis of benzodiazepine derivatives (4a–j)

A mixture of 5-acetyl-1,3-dimethylbarbituric acid **1** (1 mmol), aromatic/hetero aromatic aldehydes **2a–e** (1 mmol), 1,2-diamines **3a,b** (1 mmol) and PVP–CeO_2/rGO (30 mg) were taken in a round bottom flask (50 mL) and stirred in water at room temperature for a specified time period. The completion of the reaction was marked by TLC. The reaction mixture was kept at room temperature for a few minutes and ethyl acetate (5 mL) was added to extract the product. The catalyst being insoluble in ethyl acetate was separated by filtration, washed thoroughly with ethyl acetate (2 × 10 mL), dried and reused. The filtrate containing the crude products was washed thoroughly with double distilled water (4 × 10 mL), dried over anhydrous sodium sulphate and evaporated under reduced pressure. The crude products were recrystallized from ethanol to afford pure products **4a–j**.

3. Results and discussion

3.1. Characterization of PVP–CeO_2/rGO

The material PVP–CeO_2/rGO was synthesized as outlined in Scheme 1.

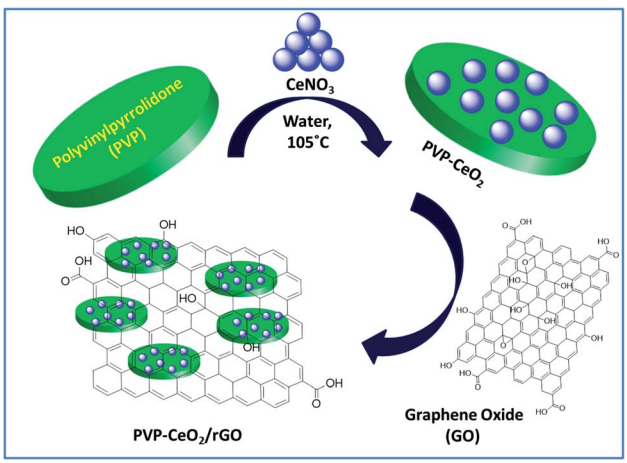

Scheme 1 Synthesis of PVP–CeO_2/rGO.

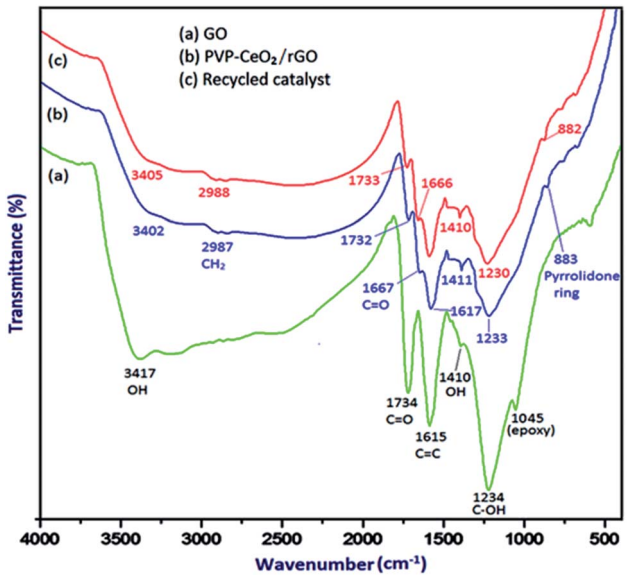

Fig. 1 FTIR spectrum of (a) GO, (b) PVP–CeO_2/rGO and (c) the recycled catalyst after six runs.

The synthesized material (PVP–CeO_2/rGO) combines the properties of PVP, CeO_2 and rGO. CeO_2 NPs provided sufficient acidity to the catalyst, PVP acted as a stabilizing agent for NPs and graphene sheets provided a surface for the catalytic activity. The material was characterized by various techniques such as FTIR, SEM, EDX, elemental mapping, TEM, Raman spectroscopy, XRD, BET, XPS and TG analyses.

3.1.1 FTIR/SEM analyses. The FTIR spectrum of GO (Fig. 1a) displayed the characteristic bands at 3417 cm^{-1}, 1734 cm^{-1}, 1615 cm^{-1}, 1410 cm^{-1}, 1234 cm^{-1} and 1045 cm^{-1} for the stretching vibration of the –OH group, C=O stretching vibration, C=C stretching vibration of aromatic rings, –OH deformation, C–OH stretching and C–O (epoxy) stretching respectively.[46] When PVP–CeO_2 was introduced into GO sheets, the intensity of C=O and C–OH bands decreased significantly whereas the band at 1045 cm^{-1} disappeared completely indicating the reduction of GO leading to the formation of PVP–CeO_2/rGO (Fig. 1b). The characteristic bands of PVP appeared at 2987 cm^{-1}, 1667 cm^{-1} and 883 cm^{-1} due to the stretching vibration of CH_2 of alkyl chain, C=O stretching and breathing vibration of the pyrrolidone ring respectively (Fig. 1b).[47] The surface morphology of GO (Fig. 2a) showed a sheet like structure, whereas the uniform distribution of PVP–CeO_2 NPs over the rGO sheets was clearly discernible in PVP–CeO_2/rGO (Fig. 2b and c).

3.1.2 EDX/elemental mapping analyses. The elemental composition of PVP–CeO_2/rGO was studied by EDX analysis and

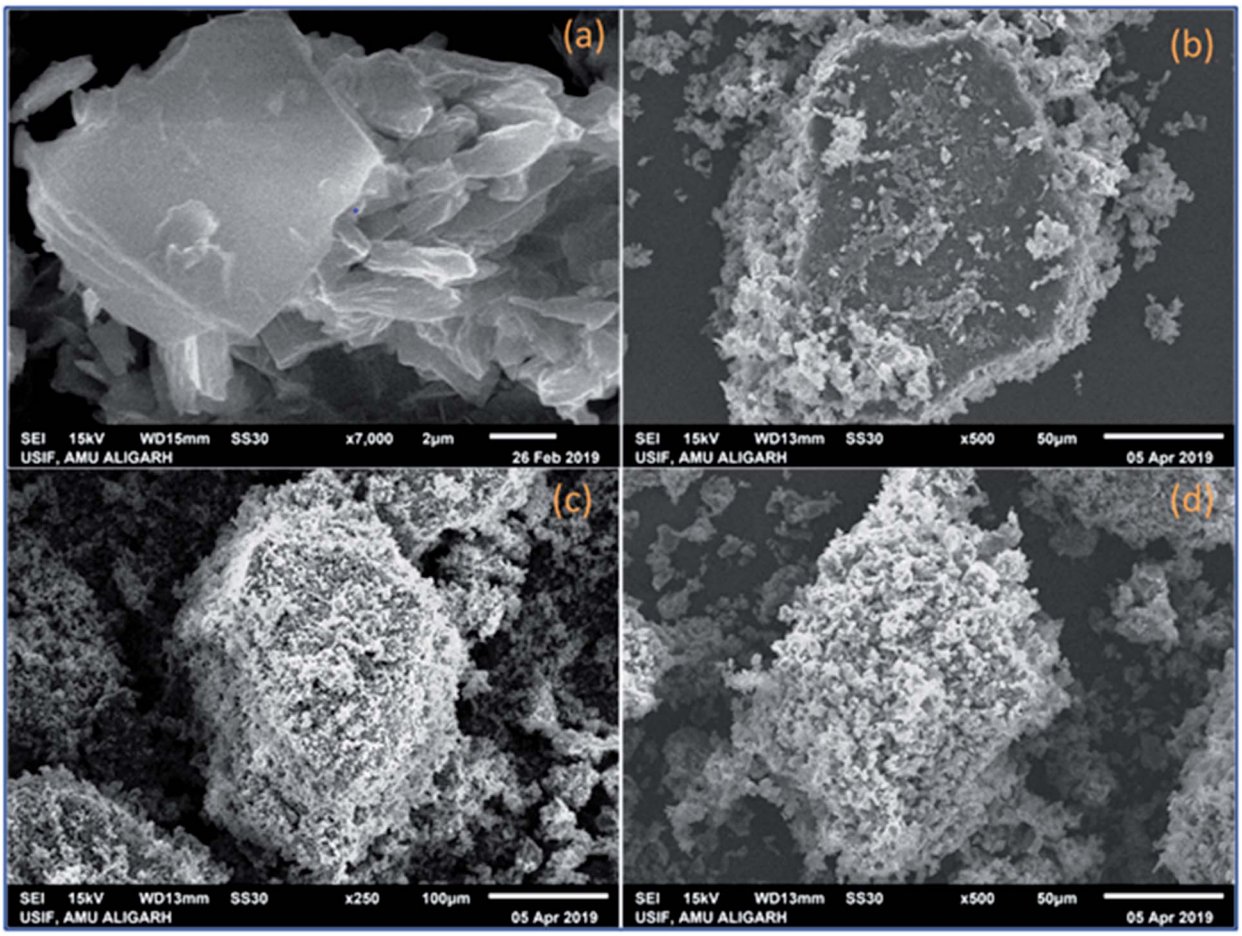

Fig. 2 SEM analysis of (a) GO, (b) PVP–CeO_2/rGO at 50 μm, (c) PVP–CeO_2/rGO at 100 μm and (d) the recycled catalyst after six runs.

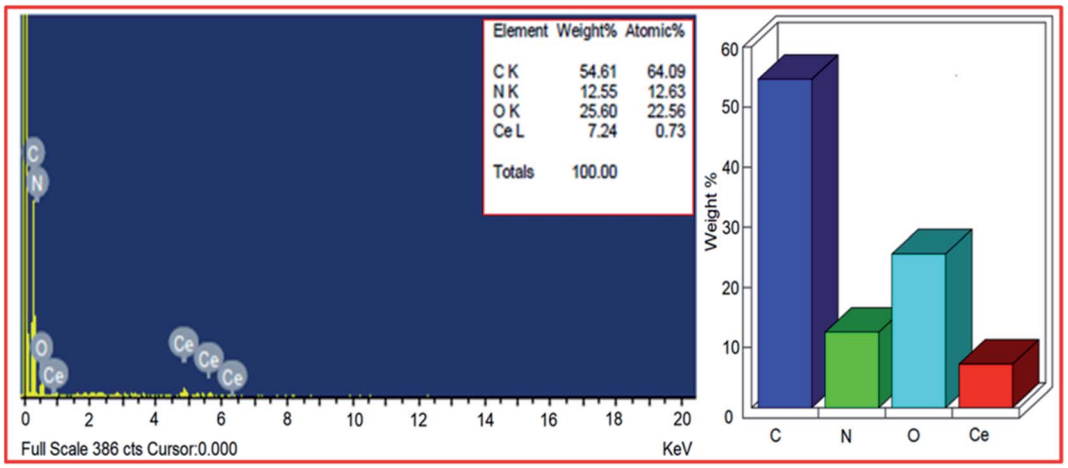

Fig. 3 Energy dispersive X-ray analysis of PVP–CeO_2/rGO.

revealed the presence of carbon, nitrogen, oxygen and cerium elements (Fig. 3). From the EDX pattern, the weight% of carbon, nitrogen, oxygen and cerium was found to be 54.61%, 12.55%, 25.60% and 7.24% respectively. In general, the carbon to oxygen ratio in GO is found to be approximately 3 : 1 [48] and in rGO most of the oxygen functionalities were removed. But, from the EDX pattern of PVP–CeO_2/rGO, the carbon : oxygen ratio was obtained to be approximately 3 : 1.5. This showed the presence of excess oxygen in PVP–CeO_2/rGO due to the incorporation of CeO_2 NPs. From the EDX pattern, the atomic% of nitrogen was obtained to be 12.63% which has come from the PVP moiety present in the catalyst. Elemental mapping analysis of PVP–CeO_2/rGO was performed to observe the distribution of the elements in the matrix. The elemental mapping image of the PVP–CeO_2/rGO material (Fig. 4a) confirmed the uniform distribution of carbon (Fig. 4b), oxygen (Fig. 4c) cerium (Fig. 4d) and nitrogen (Fig. 4e) elements in the catalyst.

3.1.3 TEM analysis. TEM analysis of GO showed a folded sheet like structure (Fig. 5a), whereas PVP–CeO_2/rGO displayed the uniform distribution of PVP–CeO_2 nanoparticles over the rGO sheets (Fig. 5b).

3.1.4 Raman analysis. Raman analysis was performed to understand the structural properties of GO and PVP–CeO_2/rGO. The presence of two characteristic broad peaks at 1360 cm^{-1} and 1591 cm^{-1} corresponds to the D and G bands of the carbon skeleton of the GO sheets (Fig. 6a).[49] After the functionalization of GO with PVP–CeO_2, a sharp characteristic peak at 462 cm^{-1} appeared due to the F_{2g} band of CeO_2 NPs[50] (Fig. 6b). The intensity of bands at 1360 cm^{-1} and 1591 cm^{-1} corresponding to the D and G bands of the carbon skeleton of GO was reduced indicating the formation of rGO (Fig. 6b).

3.1.5 XRD analysis. The characteristic peak for the GO material appeared at $2\theta = 13.3°$ corresponding to the (001) plane (Fig. 7a). This indicated the exfoliation of the GO sample

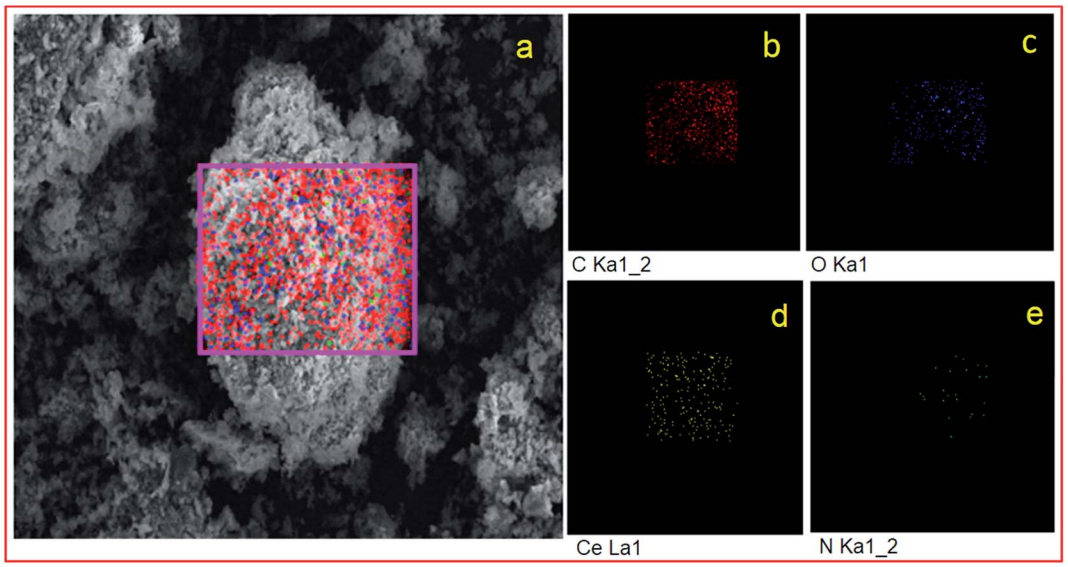

Fig. 4 Elemental mapping images of (a) PVP–CeO_2/rGO, showing the presence of (b) carbon, (c) oxygen, (d) cerium and (e) nitrogen.

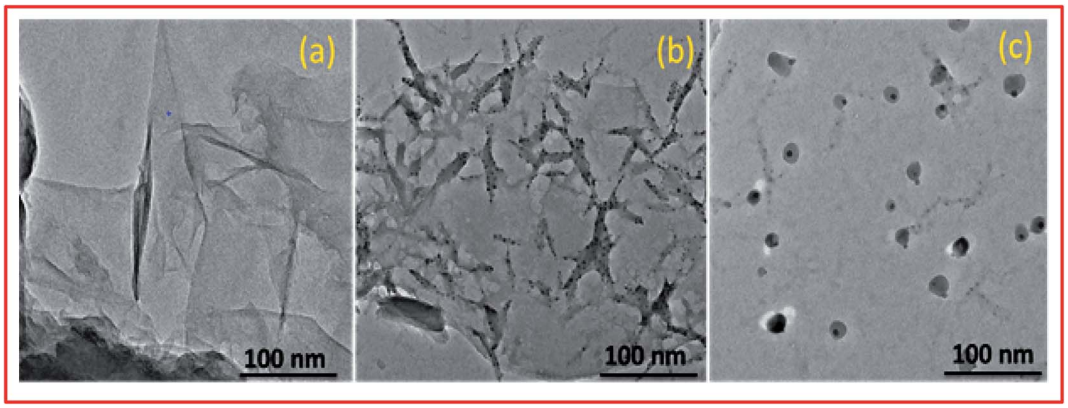

Fig. 5 TEM analysis of (a) GO, (b) PVP–CeO_2/rGO and (c) the recycled catalyst after six runs.

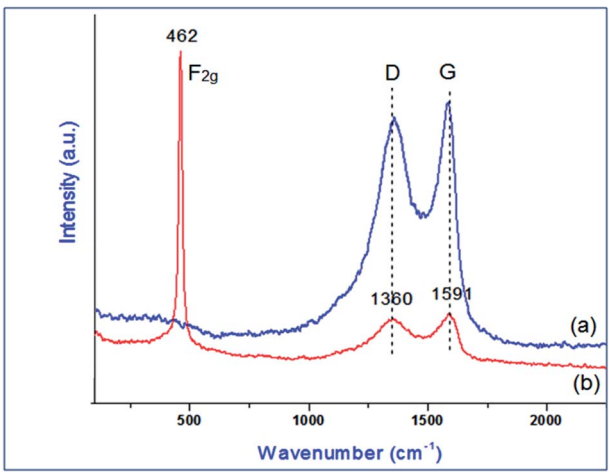

Fig. 6 Raman spectrum of (a) GO and (b) PVP–CeO_2/rGO.

and intercalation of water molecules in graphite galleries which generated oxygen functional groups in between the graphite layers upon oxidation.[51] After the functionalization of GO with PVP–CeO_2, most of the oxygen functional groups present in the GO were removed which was confirmed by the disappearance of the peak at $2\theta = 13.3°$. A strong diffraction peak at $2\theta = 23.0°$ corresponding to the (222) reflection plane was due to the presence of rGO in the catalyst.[52] The diffraction bands at $2\theta =$ 28.1, 32.1, 47.7, 55.4, 58.3, 68.8, 78.0, and 78.9 corresponding to (111), (200), (220), (311), (222), (400), (331) and (420) planes respectively were due to the presence of CeO_2 nanoparticles.[53] The presence of characteristic peaks for both rGO and CeO_2 indicates the successful formation of the desired catalytic system.

3.1.6 XPS analysis. To investigate the surface composition of different elements of the synthesized material (PVP–CeO_2/rGO), XPS analysis was carried out and the results are shown in Fig. 8. The high resolution XPS spectrum of C 1s, Ce 3d, O 1s and N 1s were also obtained (Fig. 8a–d). The C 1s showed atomic configurations of different functional groups C=C, C–O and C=O at binding energies 284.8 eV, 287.6 eV and 288.3 eV respectively[2] (Fig. 8a). The Ce 3d displayed two sharp peaks for $3d_{5/2}$ and $3d_{3/2}$ at 885.4 eV and 903.2 eV respectively[54] (Fig. 8b). The sharp bands at binding energies 534.6 eV and 402.1 eV were assigned to O 1s (Fig. 8c) and N 1s (Fig. 8d) respectively. The cerium content was found to be 7.34% which corresponds to 0.523 mmol g^{-1} of the catalyst.

3.1.7 BET analysis. Most of the catalytic properties of nanomaterials are generally associated with the surface to volume ratio; the higher the ratio, the better the catalytic activity. The measurement of the surface area and porosity of PVP–CeO_2/rGO was conducted by an adsorption/desorption experiment using BET analysis under a N_2 atmosphere (Fig. 9). The N_2 adsorption/desorption curve of PVP–CeO_2/rGO showed a surface area of 323.1098 m^2 g^{-1} confirming the porous nature of the material, and thus, providing more active sites for the catalytic activity (Fig. 9a). The pore size distribution curve exhibited a large pore volume (0.48732 cm^3 g^{-1}), which further benefited the exposure of active sites (Fig. 9b).

3.1.8 TG analysis. The TG curves of GO and PVP–CeO_2/rGO are shown in Fig. 10. The TG curve of GO (Fig. 10a) showed two

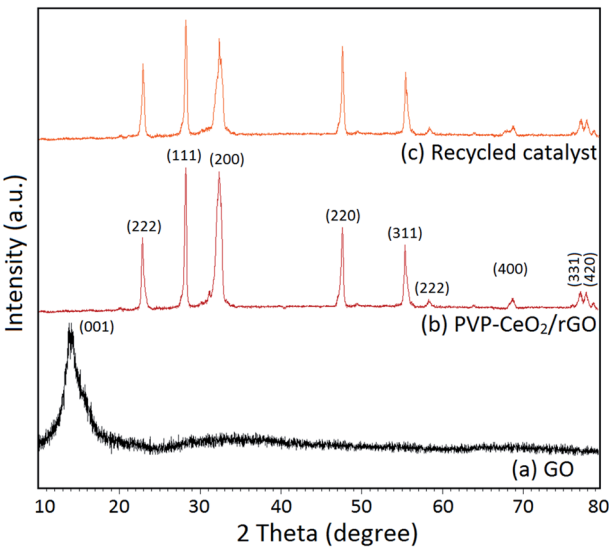

Fig. 7 XRD pattern of (a) GO, (b) PVP–CeO_2/rGO and (c) the recycled catalyst after six runs.

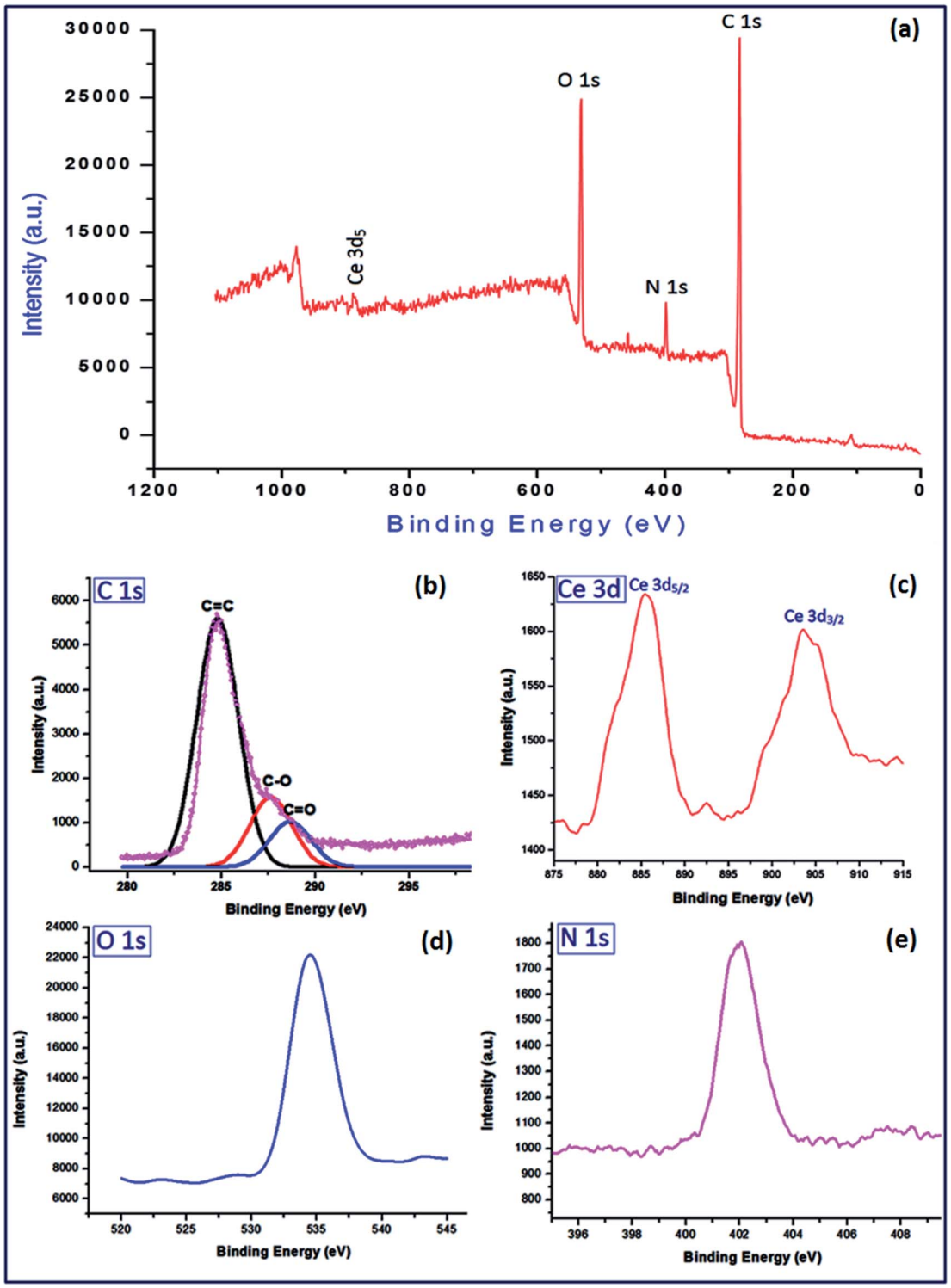

Fig. 8 XPS analysis of (a) PVP–CeO_2/rGO; survey spectrum of (b) C 1s, (c) Ce 3d, (d) O 1s and (e) N 1s.

stage weight loss at 110 °C (12.82%) and 452 °C (33.15%) due to the removal of absorbed water molecules from the GO material and decomposition of oxygen-containing functional groups respectively.[55] In the TG curve of PVP–CeO_2/rGO (Fig. 10b), the corresponding weight loss occurred at a relatively higher temperature of 635 °C (28.43%) indicating higher thermal stability of the material as compared to GO.

3.2. Catalytic evaluation

The efficiency of the synthesized material as a catalyst was tested by synthesizing benzodiazepine derivatives. Several parameters such as the effect of different catalysts, solvents, catalyst loading and temperatures on a model reaction were taken into consideration. A reaction between 5-acetyl-1,3-

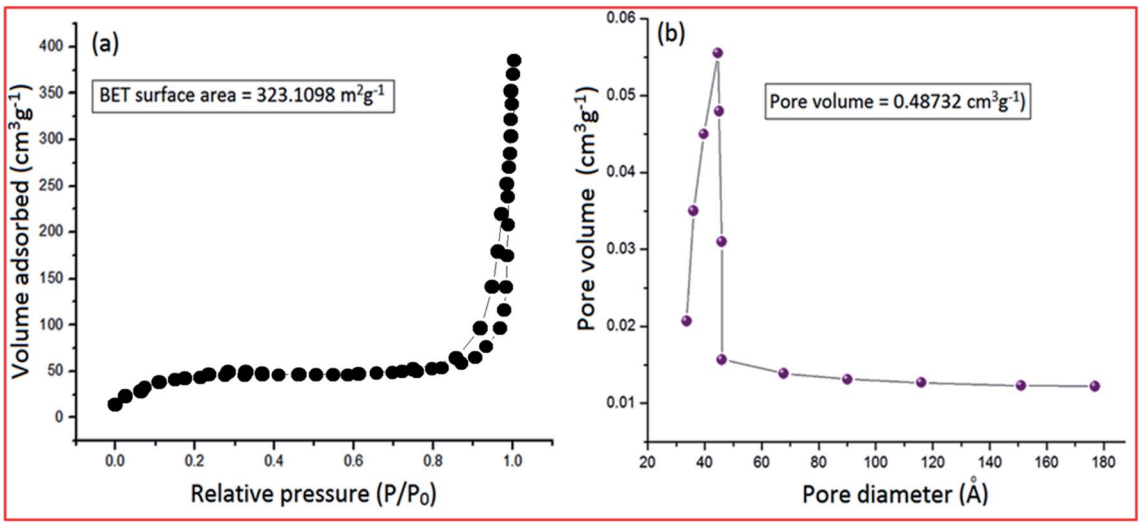

Fig. 9 (a) N_2 adsorption isotherm of PVP–CeO_2/rGO and (b) pore size distribution of PVP–CeO_2/rGO.

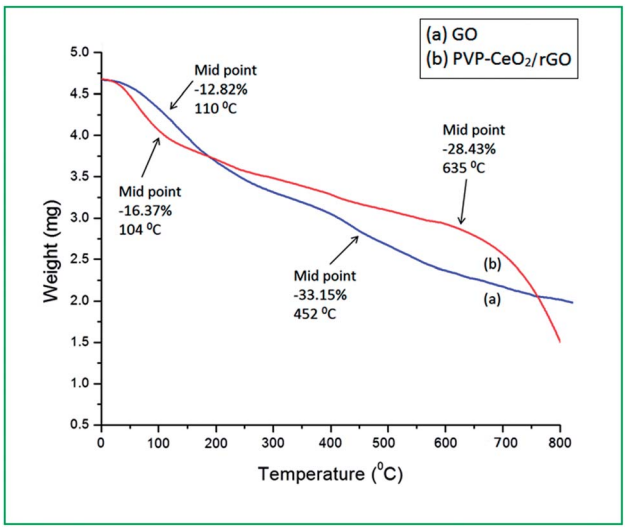

Fig. 10 TG analysis of (a) GO and (b) PVP–CeO_2/rGO.

dimethylbarbituric acid **1**, 3-nitrobenzaldehyde **2c** and *o*-phenylenediamine **3a** to produce substituted benzodiazepine **4c** was chosen as the model reaction (Scheme 2). The components **1** and **3a** had no substituents and **2c** was functionalized with a *m*-NO_2 substituent which had the minimum effect out of all aldehydes used for the synthesis of benzodiazepine derivatives. Therefore, Scheme 2, was the best composition of reactants to see the effect of different parameters.

3.2.1 Effect of different catalysts. In order to establish the superiority of our synthesized catalyst (PVP–CeO_2/rGO) for the desired transformation, different catalysts such metal oxide NPs, polymer modified metal oxide NPs and supported polymer modified metal oxide NPs were employed in the model reaction (Table 1). First, the model reaction was carried out without the catalyst and the reaction afforded no product even after 24 h (Table 1, Entry 1). Then the investigation was carried out using different metal NPs as the catalyst and the reaction afforded low to moderate yields of the product in a longer reaction time period (Table 1, Entries 2–7). Among the different metal NPs tested, CeO_2 NPs showed the best activity affording a good yield in a comparatively less reaction time period (Table 1, Entry 7). After that, the model reaction was investigated by employing different polymer modified CeO_2 NPs and the reaction showed improved results in terms of product yield and reaction time (Table 1, Entries 8–12). PVP–CeO_2 was chosen among different polymer modified CeO_2 catalysts for producing the best result (Table 1, Entry 10). Finally, PVP–CeO_2 was supported on different support materials such as Al_2O_3, ZrO_2, SiO_2 and rGO

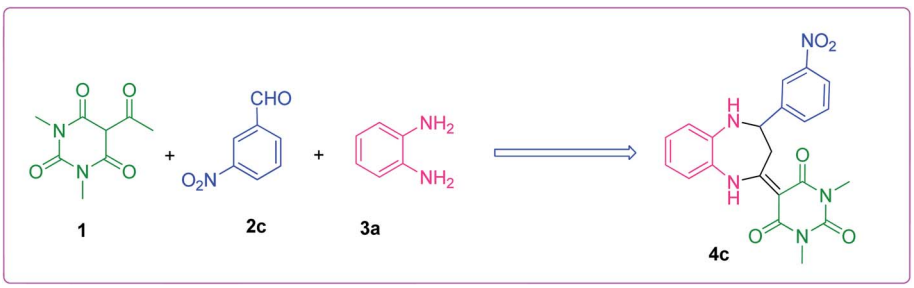

Scheme 2 Model reaction.

Table 1 Effect of different catalysts on the model reaction[a]

Entry	Catalyst	Time[b]	Yield[c] (%)
1	—	24 h	—
2	ZnO NPs	5 h	40
3	CaO NPs	4.2 h	42
4	CuO NPs	4 h	45
5	TiO_2 NPs	3.5 h	48
6	Fe_2O_3 NPs	3 h	51
7	CeO_2 NPs	2 h	54
8	PPy–CeO_2	1.8 h	56
9	PANI–CeO_2	1.5	59
10	PVA–CeO_2	1.2 h	61
11	Chitosan–CeO_2	1 h	64
12	PVP–CeO_2	50 min	70
13	PVP–CeO_2/Al_2O_3	28 min	73
14	PVP–CeO_2/ZrO_2	25 min	76
15	PVP–CeO_2/SiO_2	20 min	78
16	PVP–CeO_2/rGO	7 min	98

[a] Reaction conditions: 5-acetyl-1,3-dimethylbarbituric acid **1** (1 mmol), 3-nitrobenzaldehyde **2c** (1 mmol), *o*-phenylenediamine **3a** (1 mmol), different catalysts (30 mg), water, r.t. stirring. [b] Reaction progress monitored by TLC. [c] Isolated yield.

for the purpose of enhancing the catalytic activity (Table 1, Entries 13–16). It was observed that among the different support materials, rGO proved to be the best support material making PVP–CeO_2/rGO the best catalyst for affording the maximum yield (98%) of the product in a minimum reaction time period (7 min) (Table 1, Entry 16).

3.2.2 Effect of solvents. After finding out the most suitable catalyst, investigation was carried out to select the best solvent for the model reaction. In this effort, different protic (isopropanol, ethanol, methanol, and water) as well as aprotic (THF, ethyl acetate, acetonitrile, and acetone) solvents (Fig. 11) were employed in the model reaction. It was observed that aprotic solvents afforded a poor yield of the product in a longer reaction time period (Fig. 11, Entries 1–6), whereas protic solvents gave a satisfactory product yield (68–96%) (Fig. 11, Entries 7–10). Among different protic solvents, water proved to be the best solvent for the desired reaction affording an excellent yield (98%) of the product in minimum reaction time period (7 min) (Fig. 11, Entry 10).

3.2.3 Effect of catalyst loading. To determine the effect of different PVP–CeO_2 loadings on rGO, different loading amounts such as 10, 15, 20, 25 and 30% w/w were employed in the model reaction. It was observed that the rate of reaction increased linearly with an increased loading amount from 10–30% w/w (Fig. 12, Entries 1–5).

3.2.4 Effect of the amount of catalyst. In order to choose the optimum amount of the catalyst, the model reaction was investigated with different amounts (10, 20, 25, 30, and 40 mg) of PVP–CeO_2/rGO (Table 2, Entries 1–5). It was observed that on increasing the amount of catalyst (from 10 mg to 30 mg), the yield of the product and turnover frequency (TOF) increased from 43% to 98% and 54.81 h^{-1} to 535.37 h^{-1} respectively

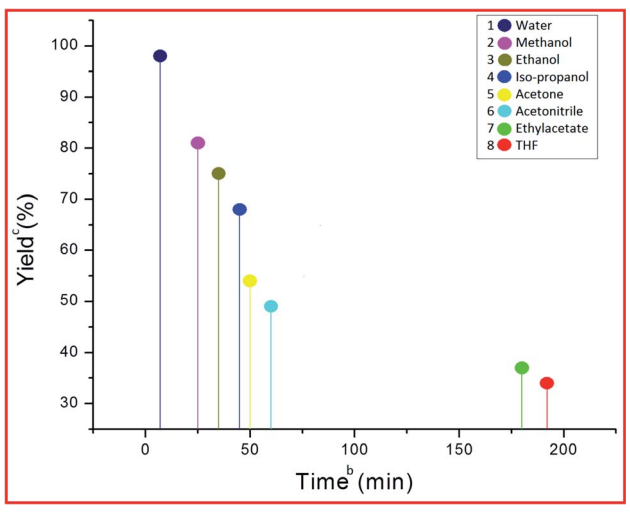

Fig. 11 Effect of different solvents on the model reaction.[a] [a]Reaction conditions: 5-acetyl-1,3-dimethylbarbituric acid **1** (1 mmol), 3-nitrobenzaldehyde **2c** (1 mmol), *o*-phenylenediamine **3a** (1 mmol), PVP–CeO_2/rGO (30 mg), solvents, r.t. stirring. [b]Reaction progress monitored by TLC. [c]Isolated yield.

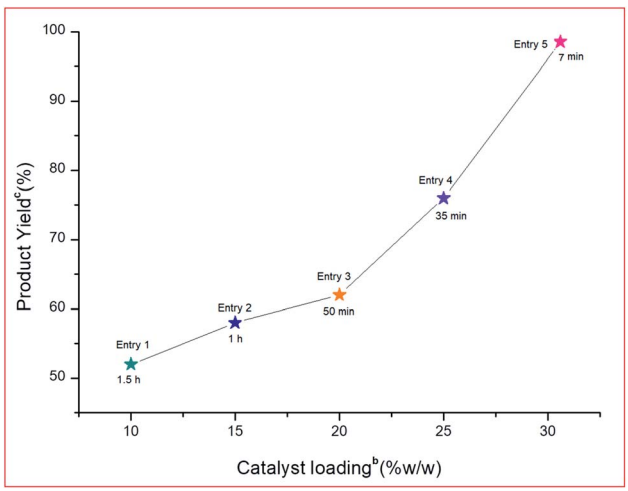

Fig. 12 Effect of different PVP–CeO_2 loadings on the support for the model reaction.[a] [a]Reaction conditions: 5-acetyl-1,3-dimethylbarbituric acid **1** (1 mmol), 3-nitrobenzaldehyde **2c** (1 mmol), *o*-phenylenediamine **3a** (1 mmol), PVP–CeO_2/rGO (30 mg), different PVP–CeO_2 loadings on support, r.t. stirring. [b]Reaction progress monitored by TLC. [c]Isolated yield.

Table 2 Effect of different amounts of the catalyst on model reaction[a]

Entry	Catalyst loading	Time[b] (min)	Yield[c] (%)	TON	TOF (h^{-1})
1	10 mg	90	43	82.21	54.81
2	20 mg	45	62	59.27	79.03
3	25 mg	25	81	61.95	148.68
4	**30 mg**	**7**	**98**	**62.46**	**535.37**
5	40 mg	7	98	46.84	401.52

[a] Reaction conditions: 5-acetyl-1,3-dimethylbarbituric acid **1** (1 mmol), 3-nitrobenzaldehyde **2c** (1 mmol), *o*-phenylenediamine **3a** (1 mmol), PVP–CeO_2/rGO, different amount of catalyst, r.t. stirring. [b] Reaction progress monitored by TLC. [c] Isolated yield.

(Table 2, Entries 1–4). This showed that the efficiency of the catalyst improved on increasing the catalyst amount. Further increasing the catalyst amount did not affect the reaction rate and hence, 30 mg of PVP–CeO_2/rGO (producing the highest TOF = 535.37 h^{-1}) was found to be the optimum amount for the desired reaction affording the maximum yield of the product

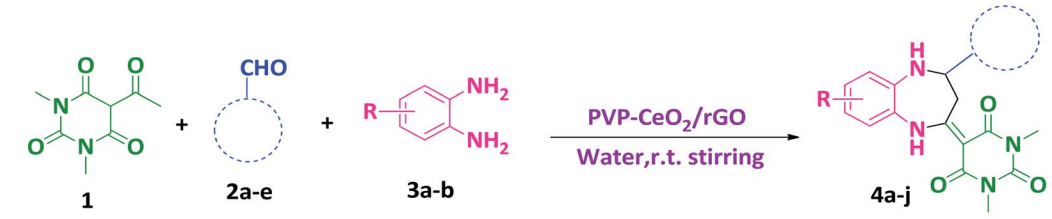

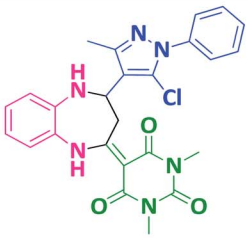
4a
8 min[b], 98%[c]

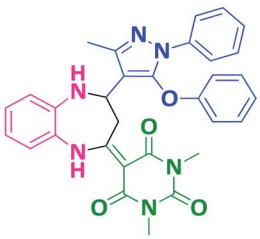
4b
8 min[b], 97%[c]

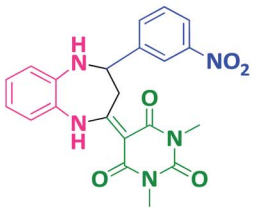
4c
7 min[b], 98 %[c]

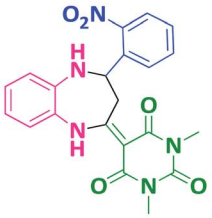
4d
9 min[b], 96 %[c]

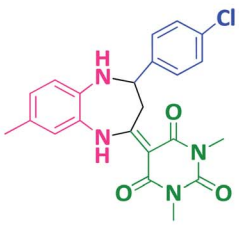
4e
7 min[b], 98 %[c]

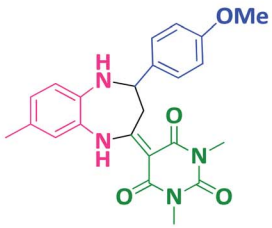
4f
8 min[b], 97 %[c]

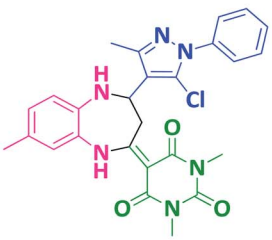
4g
8 min[b], 98 %[c]

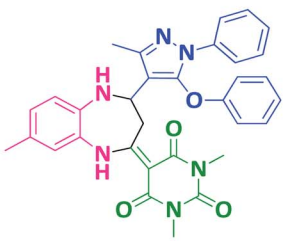
4h
9 min[b], 98 %[c]

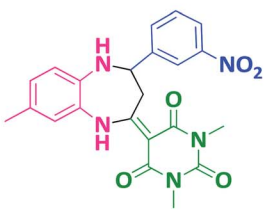
4i
8 min[b], 96 %[c]

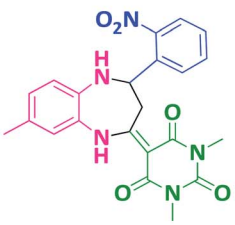
4j
8 min[b], 96 %[c]

Scheme 3 Water mediated synthesis of substituted benzodiazepine derivatives.[a] [a]Reaction conditions: **1** (1 mmol), **2a–e** (1 mmol), **3a,b** (1 mmol), PVP–CeO_2/rGO (30 mg), water, r.t. stirring. [b]Reaction progress monitored by TLC. [c]Isolated yield.

(98%) in minimum reaction time period (7 min) (Table 2, Entry 4).

3.3. Catalytic reaction

After finding out the most suitable reaction conditions, substituted benzodiazepine derivatives were synthesized by carrying out the reaction between 5-acetyl-1,3-dimethylbarbituric acid **1** (1 mmol), hetero-aromatic/aromatic aldehydes **2a–e** and 1,2-diamines **3a,b** (1 mmol) in the presence of PVP–CeO_2/rGO at room temperature stirring in water for a specified time period (Scheme 3). The turnover number (TON) and turnover frequency (TOF) of the catalyst were calculated to show the efficiency of PVP–CeO_2/rGO. The high TONs and TOFs confirmed the excellent performance of PVP–CeO_2/rGO for the synthesis of benzodiazepines (Table 3).

The single crystal structure of one of the synthesized compounds **4b** is shown in Fig. 13. The relevant details are provided in Table 4.

The green perspective of the present protocol was also discussed in terms of atom economy (AE), reaction mass efficiency (RME), overall efficiency (OE), carbon efficiency (CE), process mass intensity (PMI), E-factor and solvent intensity (SI). The details of the green metric calculations of these parameters are provided in the ESI.† The values of all parameters showed that the present protocol was fitting suitably in the range of sustainability as confirmed by an earlier study.[56] The results of the green metric parameters are given in Table 5.

Table 3 Calculation of the TON and TOF of PVP–CeO_2/rGO

Entry	Product	Time (min)	Yield (%)	TON	TOF (h^{-1})
1	**4a**	8	98	62.46	468.45
2	**4b**	8	97	61.82	463.65
3	**4c**	7	98	62.46	535.37
4	**4d**	9	96	61.18	407.86
5	**4e**	7	98	62.46	535.37
6	**4f**	8	97	61.82	463.65
7	**4g**	8	98	62.46	468.45
8	**4h**	9	98	62.46	416.40
9	**4i**	8	96	61.18	458.85
10	**4j**	8	96	61.18	458.85

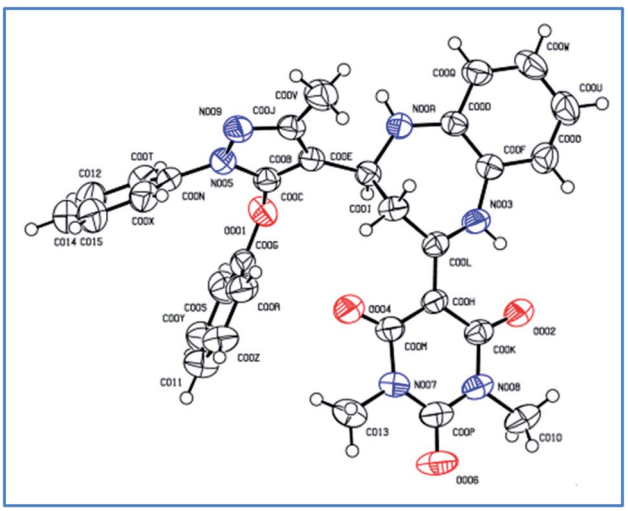

Fig. 13 ORTEP diagram of compound **4b** (ellipsoids are drawn at the 50% probability level).

Table 4 Single crystal data for compound **4b**

Identification code	**4b**
Empirical formula	$C_{31}H_{28}N_6O_4$
Formula weight	548.59
Temperature/K	273.15
Crystal system	Monoclinic
Space group	$P2_1/n$
a/Å	18.836(3)
b/Å	7.2533(10)
c/Å	19.682(3)
α/°	90
β/°	92.081(4)
γ/°	90
Volume/Å^3	2687.3(6)
Z	4
ρ_{calc}/g cm^{-3}	1.356
μ/mm^{-1}	0.093
F(000)	1152.0
Crystal size/mm^3	0.52 × 0.25 × 0.08
Radiation	MoKα (λ = 0.71073)
2Θ range for data collection/°	5.882 to 49.998
Index ranges	$-22 \le h \le 22$, $-8 \le k \le 8$, $-23 \le l \le 23$
Reflections collected	29 871
Independent reflections	4723 [R_{int} = 0.0593, R_{sigma} = 0.0407]
Data/restraints/parameters	4723/0/377
Goodness-of-fit on F^2	1.033
Final R indices $I \ge 2\sigma(I)$	R_1 = 0.0514, wR_2 = 0.1151
Final R indices all data	R_1 = 0.0943, wR_2 = 0.1372
Largest diff. peak/hole/e Å^{-3}	0.16/−0.24

3.4. Recyclability of the catalyst

The reusability of the catalyst was checked by carrying out the recycling experiment on the model reaction (ESI†). It was observed that the catalyst was efficient up to six subsequent cycles with minor loss in catalytic activity after the sixth run (Table 6 and Fig. 1S†).

The structural integrity of the recovered catalyst after six runs was established by FTIR, SEM, TEM and powder XRD analyses. In the FTIR spectrum of the recycled catalyst, characteristic peaks were observed in approximately the same region as for the fresh catalyst (Fig. 1c). The SEM and TEM images of the recovered catalyst showed a similar morphology (Fig. 2d and 5c) and characteristic peaks remained the same in the XRD pattern also (Fig. 7c).

3.5. Comparison of the activity of PVP–CeO_2/rGO with some previously reported catalysts

In order to determine the advantage of PVP–CeO_2/rGO over previously reported catalysts for the synthesis of benzodiazepines, a comparative study was carried out (Table 7). It was observed that the present methodology (Table 7, Entry 5) is

Table 5 The Green metric analysis of the synthesized compounds (4a–j)[h,i]

Compound	% yield	% AE[a]	% CE[b]	% RME[c]	% OE[d]	PMI[e]	SI[f]	E-factor[g]
4a	98	93.15	100.00	91.29	98.00	5.25	3.99	4.25
4b	97	93.83	100.00	91.01	96.99	4.86	3.53	3.86
4c	98	92.92	100.00	90.27	97.14	5.95	4.65	4.95
4d	96	92.92	100.00	88.43	95.16	6.08	4.55	5.08
4e	98	92.17	100.00	90.33	98.00	5.92	4.62	4.92
4f	97	92.10	100.00	89.34	97.00	6.03	4.61	5.03
4g	98	93.33	100.00	91.96	98.53	5.14	3.88	4.14
4h	98	93.96	100.00	92.11	98.03	4.71	3.48	3.71
4i	96	92.35	100.00	88.66	96.00	5.91	4.41	4.91
4j	96	92.35	100.00	88.66	96.00	5.91	4.41	4.91

[a] % AE: percentage atom economy. [b] % CE: percentage carbon efficiency. [c] % RME: percentage reaction mass efficiency. [d] % OE: percentage overall efficiency. [e] PMI: process mass intensity. [f] SI: solvent intensity. [g] E-factor. [h] Catalyst amount was not used in the calculations because of its reusability.[57] [i] Calculations up to the crude product in all cases.

Table 6 Recycling study of the catalyst for the model reaction[a]

Catalytic cycle	Time[b] (min)	Yield[c] (%)
1	7	98
2	7	98
3	7	98
4	7	98
5	7	98
6	7	98
7	7	90

[a] Reaction conditions: 5-acetyl-1,3-dimethylbarbituric acid **1** (1 mmol), 3-nitrobenzaldehyde **2c** (1 mmol), *o*-phenylenediamine **3a** (1 mmol), PVP–CeO_2/rGO(30 mg), water, r.t. stirring. [b] Reaction progress monitored by TLC. [c] Isolated yield.

Table 7 Comparison of the catalytic performance of PVP–CeO_2/rGO with reported catalysts

Entry	Catalyst	Solvent	Temperature	Time	% yield (maximum)	Ref.
1	[H-NMP][HSO_4]	EtOH	100 °C	15 min	85	58
2	$FeCl_3$–SiO_2	EtOH	0 °C	2 h	95	59
3	Nano-γ-Fe_2O_3–SO_3H	Solvent-free	90 °C	2 h	90	60
4	NiO–SiO_2 NCs	EtOH	70 °C	10 min	98	61
5	**PVP–CeO_2/rGO**	**Water**	**r.t.**	**7 min**	**98**	**This work**

better as compared with other reported methods (Table 7, Entries 1–4) in terms of product yield and time. The use of water as a solvent and room temperature synthesis make it environment friendly as well.

4. Conclusion

We have developed a simple and easy route for the reduction of graphene oxide with the help of PVP–CeO_2 NPs. The carbonaceous material, PVP–CeO_2/rGO, was used as a heterogeneous catalyst for the multicomponent synthesis of benzodiazepines. The high catalytic performance of the carbon material was verified by its excellent product yield (96–98%), short reaction time period (7–10 min) and recyclability. The methodology involved use of non-toxic chemicals and solvents for the synthesis and therefore can be considered as eco-friendly.

Conflicts of interest

There is no conflict of interest to declare.

Acknowledgements

The authors would like to acknowledge DRS-II New Delhi for providing necessary research facilities and USIF, A.M.U. for facilitating SEM/EDX, elemental mapping, and TEM analyses and SAIF, IIT-Patna for single crystal X-ray crystallographic analysis.

References

1 K. S. Novoselov, V. I. Fal, L. Colombo, P. R. Gellert, M. G. Schwab and K. Kim, *Nature*, 2012, **490**, 192.
2 Q. Lyu, H. Yan, L. Li, Z. Chen, H. Yao and Y. Nie, *Polymers*, 2017, **9**, 447.
3 K. S. Novoselov, A. K. Geim, S. V Morozov, D. Jiang, Y. Zhang, S. V Dubonos, I. V Grigorieva and A. A. Firsov, *Science*, 2004, **306**, 666–669.
4 K. S. Kim, Y. Zhao, H. Jang, S. Y. Lee, J. M. Kim, K. S. Kim, J.-H. Ahn, P. Kim, J.-Y. Choi and B. H. Hong, *Nature*, 2009, **457**, 706.
5 S. Stankovich, D. A. Dikin, R. D. Piner, K. A. Kohlhaas, A. Kleinhammes, Y. Jia, Y. Wu, S. T. Nguyen and R. S. Ruoff, *Carbon*, 2007, **45**, 1558–1565.
6 H. Shin, K. K. Kim, A. Benayad, S. Yoon, H. K. Park, I. Jung, M. H. Jin, H. Jeong, J. M. Kim and J. Choi, *Adv. Funct. Mater.*, 2009, **19**, 1987–1992.

7 S. Stankovich, D. A. Dikin, G. H. B. Dommett, K. M. Kohlhaas, E. J. Zimney, E. A. Stach, R. D. Piner, S. T. Nguyen and R. S. Ruoff, *Nature*, 2006, **442**, 282.
8 G. Wang, J. Yang, J. Park, X. Gou, B. Wang, H. Liu and J. Yao, *J. Phys. Chem. C*, 2008, **112**, 8192–8195.
9 R. Yin, P. Shen and Z. Lu, *J. Colloid Interface Sci.*, 2019, **550**, 110–116.
10 R. Wijaya, G. Andersan, S. P. Santoso and W. Irawaty, *Sci. Rep.*, 2020, **10**, 1–9.
11 R. Sha and S. Badhulika, *J. Electroanal. Chem.*, 2018, **816**, 30–37.
12 L. Gan, B. Li, Y. Chen, B. Yu and Z. Chen, *Chemosphere*, 2019, **219**, 148–154.
13 W. Zhu, W. Liu, T. Li, X. Yue, T. Liu, W. Zhang, S. Yu, D. Zhang and J. Wang, *Electrochim. Acta*, 2014, **146**, 419–428.
14 D. Zhang, X. Liu and X. Wang, *J. Inorg. Biochem.*, 2011, **105**, 1181–1186.
15 A. H. Al-Marri, M. Khan, M. R. Shaik, N. Mohri, S. F. Adil, M. Kuniyil, H. Z. Alkhathlan, A. Al-Warthan, W. Tremel and M. N. Tahir, *Arabian J. Chem.*, 2016, **9**, 835–845.
16 B. Amanulla, S. Palanisamy, S.-M. Chen, V. Velusamy, T.-W. Chiu, T.-W. Chen and S. K. Ramaraj, *J. Colloid Interface Sci.*, 2017, **487**, 370–377.
17 F.-Y. Kong, S.-X. Gu, J.-Y. Wang, H.-L. Fang and W. Wang, *Sens. Actuators, B*, 2015, **213**, 397–403.
18 N. Meng, J. Cheng, Y. Zhou, W. Nie and P. Chen, *Appl. Surf. Sci.*, 2017, **396**, 310–318.
19 N. Pachauri, K. Dave, A. Dinda and P. R. Solanki, *J. Mater. Chem. B*, 2018, **6**, 3000–3012.
20 C. R. Stanek, A. H. H. Tan, S. L. Owens and R. W. Grimes, *J. Mater. Sci.*, 2008, **43**, 4157–4162.
21 S. Liu, Z. Chen, N. Zhang, Z.-R. Tang and Y.-J. Xu, *J. Phys. Chem. C*, 2013, **117**, 8251–8261.
22 Y. Pan, S. Wang, C. W. Kee, E. Dubuisson, Y. Yang, K. P. Loh and C.-H. Tan, *Green Chem.*, 2011, **13**, 3341–3344.
23 H. A. Elazab, A. R. Siamaki, S. Moussa, B. F. Gupton and M. S. El-Shall, *Appl. Catal., A*, 2015, **491**, 58–69.
24 S. Verma, D. Verma, A. K. Sinha and S. L. Jain, *Appl. Catal., A*, 2015, **489**, 17–23.
25 Q. M. Kainz, R. Linhardt, R. N. Grass, G. Vilé, J. Pérez-Ramírez, W. J. Stark and O. Reiser, *Adv. Funct. Mater.*, 2014, **24**, 2020–2027.
26 (*a*) A. V. Kumar and K. R. Rao, *Tetrahedron Lett.*, 2011, **52**, 5188–5191; (*b*) T. Wu, X. Wang, H. Qiu, J. Gao, W. Wang and Y. Liu, *J. Mater. Chem.*, 2012, **22**, 4772–4779.
27 T. Hoshino, Y. Kurata, Y. Terasaki and K. Susa, *J. Non-Cryst. Solids*, 2001, **283**, 129–136.
28 P. B. Zantye, A. Kumar and A. K. Sikder, *Mater. Sci. Eng., R*, 2004, **45**, 89–220.
29 M. J. Cumbo, D. Fairhurst, S. D. Jacobs and B. E. Puchebner, *Appl. Opt.*, 1995, **34**, 3743–3755.
30 V. Sajith, C. B. Sobhan and G. P. Peterson, *Adv. Mech. Eng.*, 2010, **2**, 581407.
31 (*a*) L. Vivier and D. Duprez, *ChemSusChem*, 2010, **3**, 654–678; (*b*) M. Tamura, K. Shimizu and A. Satsuma, *Chem. Lett.*, 2012, **41**, 1397–1405.
32 S. V Jadhav, D. S. Nikam, V. M. Khot, N. D. Thorat, M. R. Phadatare, R. S. Ningthoujam, A. B. Salunkhe and S. H. Pawar, *New J. Chem.*, 2013, **37**, 3121–3130.
33 G. Lu, S. Li, Z. Guo, O. K. Farha, B. G. Hauser, X. Qi, Y. Wang, X. Wang, S. Han and X. Liu, *Nat. Chem.*, 2012, **4**, 310.
34 M. Bahadory, PhD thesis, Drexler University, USA, 2008.
35 R. Si, Y.-W. Zhang, L.-P. You and C.-H. Yan, *J. Phys. Chem. B*, 2006, **110**, 5994–6000.
36 M. Di Braccio, G. C. Grossi, G. Roma, L. Vargiu, M. Mura and M. E. Marongiu, *Eur. J. Med. Chem.*, 2001, **36**, 935–949.
37 J. R. Kavali and B. V. Badami, *Il Farmaco*, 2000, **55**, 406–409.
38 A. Kamal, N. Shankaraiah, S. Prabhakar, C. R. Reddy, N. Markandeya, K. Laxma and X. Devaiah, *Bioorg. Med. Chem. Lett.*, 2008, **18**, 2434–2439.
39 L. Kosychova, L. Pleckaitiene, Z. Staniulyte, R. Janciene, A. Palaima and B. D. Puodziunaite, *Arkivoc*, 2006, (xiii), 158–164.
40 L. Kosychova, Z. Stumbreviciute, L. Pleckaitiene, R. Janciene and B. D. Puodziunaite, *Chem. Heterocycl. Compd.*, 2004, **40**, 811–815.
41 X. Che, L. Zheng, Q. Dang and X. Bai, *Tetrahedron*, 2006, **62**, 2563–2568.
42 M.-O. Simon and C.-J. Li, *Chem. Soc. Rev.*, 2012, **41**, 1415–1427.
43 (*a*) S. Siddiqui, M. U. Khan and Z. N. Siddiqui, *ACS Sustainable Chem. Eng.*, 2017, **5**, 7932–7941; (*b*) S. Siddiqui and Z. N. Siddiqui, *Catal. Lett.*, 2018, **148**, 3628–3645; (*c*) S. Siddiqui and Z. N. Siddiqui, *Appl. Organomet. Chem.*, 2019, **33**, e5161; (*d*) M. U. Khan and Z. N. Siddiqui, *ACS Omega*, 2018, **3**, 10357–10364; (*e*) M. U. Khan, S. Siddiqui and Z. N. Siddiqui, *ACS Omega*, 2019, **4**, 7586–7595; (*f*) R. A. Rather and Z. N. Siddiqui, *J. Organomet. Chem.*, 2018, **868**, 164–174; (*g*) R. A. Rather and Z. N. Siddiqui, *RSC Adv.*, 2019, **9**, 15749–15762.
44 M. Kooti and M. Afshari, *Mater. Res. Bull.*, 2012, **47**, 3473–3478.
45 R. C. Merrifield, Z. W. Wang, R. E. Palmer and J. R. Lead, *Environ. Sci. Technol.*, 2013, **47**, 12426–12433.
46 S. Lv, Q. Zhou, Y. Cui, W. Yang and Y. Li, *Arabian J. Chem.*, 2019, **12**, 3028–3037.
47 Y.-J. Song, M. Wang, X.-Y. Zhang, J.-Y. Wu and T. Zhang, *Nanoscale Res. Lett.*, 2014, **9**, 17.
48 I. Tiginyanu, V. Ursaki and V. Popa, Ultra-thin membranes for sensor applications, in *Nanocoatings and Ultra-Thin Films*, Woodhead Publishing, 2011, pp. 330–354.
49 I. Boukhoubza, M. Khenfouch, M. Achehboune, L. Leontie, A. Carlescu, C. Doroftei, B. M. Mothudi, I. Zorkani and A. Jorio, *J. Alloys Compd.*, 2020, 154874.
50 P. Sudarsanam, B. Mallesham, D. N. Durgasri and B. M. Reddy, *RSC Adv.*, 2014, **4**, 11322–11330.
51 P. Chamoli, M. K. Das and K. K. Kar, *J. Phys. Chem. Solids*, 2018, **113**, 17–25.
52 M. J. McAllister, J.-L. Li, D. H. Adamson, H. C. Schniepp, A. A. Abdala, J. Liu, M. Herrera-Alonso, D. L. Milius, R. Car and R. K. Prud'homme, *Chem. Mater.*, 2007, **19**, 4396–4404.
53 S. Wang, F. Gao, Y. Zhao, N. Liu, T. Tan and X. Wang, *Nanoscale Res. Lett.*, 2018, **13**, 377.

54 E. Bêche, P. Charvin, D. Perarnau, S. Abanades and G. Flamant, *Surf. Interface Anal.*, 2008, **40**, 264–267.
55 P. Chamoli, M. K. Das and K. K. Kar, *Phys. E*, 2017, **90**, 76–84.
56 M. M. Khan, S. Khan, S. Shareef and S. C. Sahoo, *RSC Adv.*, 2018, **8**, 41892–41903.
57 J. Safari, S. H. Banitaba and S. D. Khalili, *J. Mol. Catal. A: Chem.*, 2011, **335**, 46–50.
58 H. Naeimi and H. Foroughi, *Chin. J. Catal.*, 2015, **36**, 734–741.
59 Y. S. An, X. Q. Li, X. R. An and L. Z. Wang, *Monatsh. Chem.*, 2015, **146**, 165–172.
60 A. Amoozadeh, M. Malmir, N. Koukabi and S. Otokesh, *J. Chem. Res.*, 2015, **39**, 694–697.
61 Z. Nasir, A. Ali, M. Shakir, R. Wahab, Shamsuzzaman and Lutfullah, *New J. Chem.*, 2016, **40**, 4223–4227.